

Low-frequency Noise Figures-of-merit in RF SiGe HBT Technology

Jin Tang, Guofu Niu, Zhenrong Jin, John D. Cressler, Shiming Zhang, Alvin J. Joseph¹, and David L. Harame¹

ECE Department, 200 Broun Hall, Auburn University, Auburn, AL 36849, USA

Tel: 334 844-1856 / Fax: 334 844-1888 / E-mail: tangjin@eng.auburn.edu

¹IBM Microelectronics, Essex Junction, VT 05452, USA

Abstract—We present the first systematic experimental and modeling results of corner frequency (f_C) and the corner frequency to cutoff frequency ratio (f_C/f_T) for SiGe HBTs in a commercial SiGe RF technology. The f_C/f_T ratio is examined as a function of biasing current for SiGe HBTs featuring multiple collector doping profiles (breakdown voltages) and multiple SiGe profiles.

I. INTRODUCTION

SiGe HBT technology has come of age as an important semiconductor technology for both wireless and wired telecommunication applications, because of its superior analog and RF performance, and its CMOS integration capability [1]. One of the advantages of SiGe HBTs over GaAs HBTs is the low $1/f$ noise [2], making them excellent choices for low-noise amplifiers, oscillators [3], and power amplifiers. Traditionally, $1/f$ noise is characterized by the corner frequency f_C , at which the $1/f$ noise equals the white noise. This, however, does not take into account transistor frequency response, and is thus not suitable for assessing transistor capability for applications such as oscillators. Si BJTs typically have low f_C , but do not have sufficient gain to sustain oscillation at RF and microwave frequencies because of their limited f_T . GaAs HBTs have high f_T , but typically have high f_C and hence generate larger phase noise when used in oscillators. SiGe HBTs, however, provide f_T comparable to GaAs HBTs, and lower f_C than Si BJTs (as shown below), making them an attractive choice for ultra-low phase noise oscillators. A better figure-of-merit to measure transistor $1/f$ noise for oscillator application is the f_C/f_T ratio recently proposed in [4], since it takes into account transistor frequency response through f_T .

This work presents a systematic investigation of the two $1/f$ noise figures-of-merit f_C and f_C/f_T in a commercial SiGe technology. The impact of biasing collector current density, SiGe profile design, and collector doping profile on both f_C and f_C/f_T are examined using extensive measurements. Analytical models of f_C and f_C/f_T are derived and verified using experimental data. These results are important for optimal transistor biasing in RFIC design as well as for SiGe profile optimization in device design.

II. DEVICE TECHNOLOGY

Fig. 1 shows a schematic cross-section of the SiGe HBT used in this work. The SiGe HBT has a planar, self-aligned structure with a conventional poly emitter contact, silicided extrinsic base, and deep- and shallow-trench isolation. The SiGe base was grown using the UHV/CVD technique. Devices of two different breakdown voltages were obtained on the same chip in the same fabrication flow by selective implantation during collector formation. The

standard breakdown voltage (SBV) devices received both a deep and a shallow collector implant, and have a peak f_T of 50GHz ($BV_{CEO} = 3.3V$). The high breakdown voltage (HBV) devices received only the deep collector implant, and have a peak f_T of 30GHz ($BV_{CEO} = 5.3V$). Details of the fabrication process can be found in [5].

Four wafers with different SiGe base profile designs were measured, including a 10% peak SiGe control, a 14% peak low-noise design (LN1), a 18% peak low-noise design (LN2), and a Si BJT comparison. Details of the SiGe profile design can be found in [6]–[7]. All of the wafers were fabricated in the same wafer lot under identical processing conditions. The SiGe films in all of the SiGe designs are unconditionally stable. Compared to the SiGe control, the LN1 and LN2 designs have a higher Ge content and a larger Ge gradient in the neutral base to achieve higher β and higher f_T , but less Ge retrograding into the collector to keep the total Ge content within the thermal stability limit.

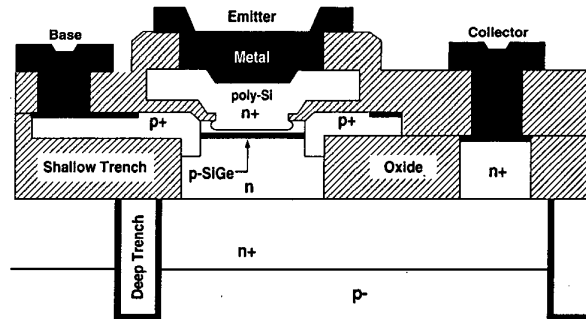


Fig. 1. Schematic cross section of the SiGe HBTs used in this work.

III. FIGURES-OF-MERIT

It has been experimentally established that the major $1/f$ noise source in these SiGe HBTs is the base current $1/f$ noise [2] [3]. The $1/f$ noise is proportional to I_B^α and the inverse of the emitter area A_E :

$$S_{I_B} = \frac{K}{A_E} I_B^\alpha \frac{1}{f} \quad (1)$$

where K is a technology dependent constant, and $\alpha \approx 2$ for typical SiGe HBTs. K/A_E is also known as the flicker noise constant K_F in SPICE. The corner frequency f_C is obtained by equating S_{I_B} to

$2qI_B$:

$$f_C = \frac{KI_B}{2qA_E} = \frac{KJ_C}{2q\beta} \quad (2)$$

where $\alpha \approx 2$ is used, J_C is the collector current density, and β is the current gain. The AC β was assumed to be the same as the DC β for simplicity, and the error introduced is negligible for these devices. Eq. (2) suggests that f_C is proportional to J_C and K , and inversely proportional to β . This differs from that derived in [4]. The derivation of [4] showed that f_C is independent of biasing current density, because $\alpha = 1$ was assumed according to mobility fluctuation. This, however, is not the case in our devices, which all show an α close to 2.

The figure-of-merit for frequency response, cutoff frequency f_T , is related to J_C by:

$$\begin{aligned} \frac{1}{2\pi f_T} &\approx \tau_f + \frac{1}{g_m} C_t \\ &= \tau_f + \frac{V_t}{J_C} C_t \end{aligned} \quad (3)$$

where τ_f is the forward transit time, $g_m = J_C/V_t$ is the transconductance per unit area, and C_t is the total junction depletion capacitance per unit area. Prior to f_T rolloff at high J_C , τ_f and C_t are constants in the typical J_C range of interest to RF circuits (0.1–1.5mA/ μm^2). The f_C/f_T ratio is obtained by combining (2) and (3):

$$\begin{aligned} \frac{f_C}{f_T} &= K \frac{\pi}{q} \frac{J_C}{\beta} \left(\tau_f + V_t \frac{C_t}{J_C} \right) \\ &= \frac{K\pi}{\beta q} \left(\tau_f J_C + V_t C_t \right) \end{aligned} \quad (4)$$

The model thus suggests a *linear* increase of the f_C/f_T ratio with operating collector current density J_C provided that β and τ_f are constants. This is in contrast to the prediction of a J_C independent f_C/f_T ratio in [4], which assumed $\alpha = 1$ ($\alpha \approx 2$ in our devices). At higher J_C where f_T is larger, $\tau_f J_C \gg V_t C_t$, and $f_C/f_T \approx K\pi\tau_f J_C/\beta q$. The f_C/f_T ratio is thus determined by the $K\tau_f/\beta$ term at higher J_C . A smaller τ_f , a higher β , and a smaller K factor are desired to reduce f_C/f_T . A smaller f_C/f_T indicates better phase noise performance at higher frequencies.

IV. EXPERIMENTAL RESULTS

Low-frequency noise spectra and s-parameters were measured on both standard and high breakdown voltage devices for the SiGe control, the LN1 and LN2 low-noise SiGe designs, and the Si comparison. Low-frequency noise was measured using an EG&G 5113 preamplifier and an HP3561A dynamic signal analyzer controlled by a Labview program. S-parameters were measured from 0.5 to 40GHz using an HP8510C vector network analyzer, from which f_T was extracted. The forward transit time τ_f and the depletion capacitance per unit area C_t were determined from the intercept and slope of the linear extrapolation of the measured $1/f_T - 1/J_C$ data, respectively. In the low-frequency noise measurements, devices were biased at collector current densities from 0.1–1.5mA/ μm^2 , the range of interest to RF circuits for the standard breakdown voltage devices.

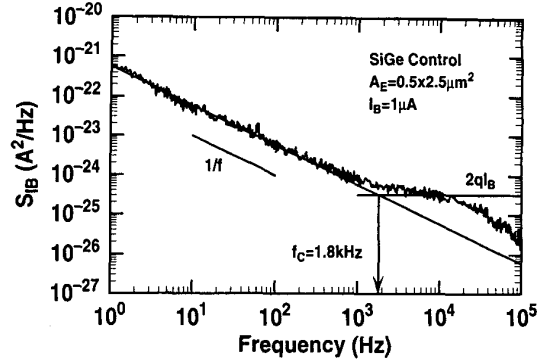


Fig. 2. A typical low-frequency noise spectrum of SiGe HBT used in this work. $A_E = 0.5 \times 2.5 \mu\text{m}^2$. $I_B = 1 \mu\text{A}$.

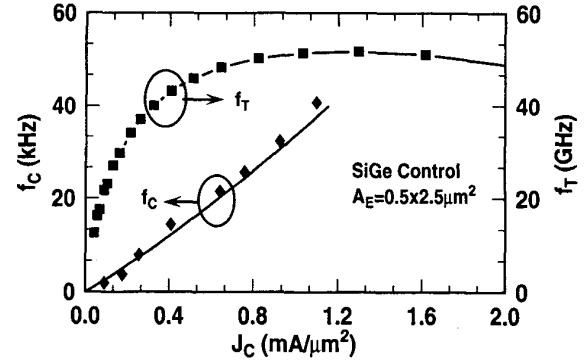


Fig. 3. Measured corner frequency f_C and cutoff frequency f_T as a function of J_C for the standard breakdown voltage SiGe control HBT. $A_E = 0.5 \times 2.5 \mu\text{m}^2$.

Fig. 2 shows a typical low-frequency base current noise spectrum (S_{I_B}) for a standard breakdown voltage (SBV) SiGe control HBT. The noise spectrum shows a clear $1/f$ component and the $2qI_B$ shot noise level. The corner frequency f_C is determined from the intercept of the $1/f$ component and the $2qI_B$ shot noise level. The rolloff above 10kHz is due to the bandwidth limitation of the preamplifier used. The measured $S_{I_B} \times f$ product was plotted as a function of I_B , from which the SPICE $1/f$ noise constant K_F was extracted. $S_{I_B} \propto I_B^\alpha$, and α is close to 2 in all cases. The obtained K_F is approximately proportional to $1/A_E$, leading to an emitter area independent K factor of $1.0 \times 10^{-9} \mu\text{m}^2$. The measured K factor is approximately the same for all of the SiGe designs.

A. J_C Dependence

The measured and calculated f_C versus J_C are shown on the left y-axis of Fig. 3 for a standard breakdown voltage HBT on the SiGe control wafer. The measured f_T versus J_C dependence is shown on the right y-axis. The corner frequency f_C increases with J_C , as predicted by (2). The calculated f_C are in close agreement with measured data. The slight deviation from a linear increase results from the J_C dependence of β . The cutoff frequency f_T increases with J_C according to (3) prior to the high injection f_T rolloff.

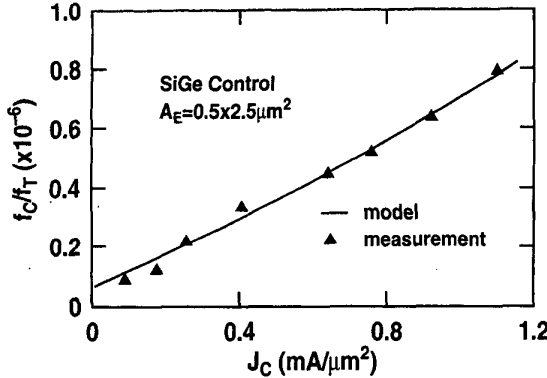


Fig. 4. Measured and modeled f_C/f_T ratio as a function of J_C for the standard breakdown voltage SiGe control HBT. $A_E = 0.5 \times 2.5 \mu\text{m}^2$.

Fig. 4 shows the measured f_C/f_T ratio, together with modeling results calculated using (4). The modeling results agree well with the measured data. The f_C/f_T ratio increases with J_C , as predicted by (4).

B. Collector Doping Dependence

SiGe BiCMOS is a promising technology for developing state-of-the-art power amplifiers with fully integrated bias- and power-control circuitry. The SiGe technology under study offers both high f_T and high breakdown voltage devices on the same chip, and the high breakdown voltage devices were optimized for power amplifiers. A logical question is how does the collector doping profile affect the $1/f$ noise, the corner frequency f_C , and the f_C/f_T ratio?

Fig. 5 compares the $S_{I_B} \times f$ product as a function of I_B for standard and high breakdown voltage devices on the SiGe control wafer. At the same I_B , the standard and high breakdown voltage devices show nearly the same $S_{I_B} \times f$ product. This translates into nearly identical f_C under the same J_C because of similar β in both devices.

Fig. 6 compares f_C as a function of J_C for the standard and high breakdown voltage devices. The modeling results (lines) agree

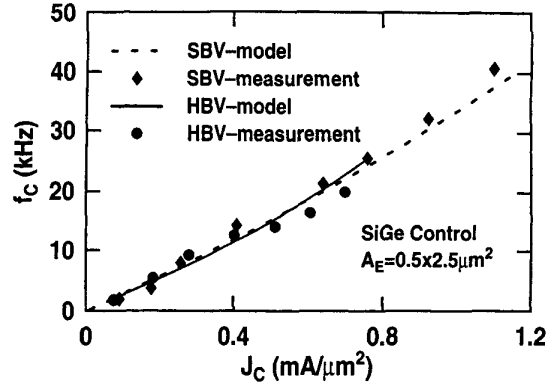


Fig. 6. Measured and modeled f_C as a function of J_C for the standard and high breakdown voltage SiGe control HBTs.

well with the measured data (symbols). Fig. 7 shows the measured and modeled f_C/f_T ratio versus J_C , together with measured f_T for both devices. At lower J_C , the f_C/f_T ratio is nearly identical in the standard and high breakdown voltage devices. At higher J_C , the f_C/f_T ratio becomes higher in the high breakdown voltage device because of the lower f_T caused by the enhanced Kirk effect at lower collector doping.

C. SiGe Profile Dependence

The two low-noise profiles, LN1 and LN2, were optimized to improve β , f_T and NF_{min} without sacrificing SiGe film stability and peak f_T [6]-[7]. The $1/f$ noise K factor is nearly identical for all of the SiGe designs. We thus expect a significant reduction of f_C as well as f_C/f_T in the two low-noise SiGe designs according to (2) and (4).

The measured f_C is indeed the lowest in LN1 and LN2, and highest in the Si BJT, as shown in Fig. 8. All of the SiGe HBTs have much higher f_T than the Si BJT, as shown in Fig. 9. LN1 and LN2 have a slightly higher f_T than the SiGe control. The f_C/f_T ratio is the lowest in the two low-noise HBT designs, because of much lower f_C and slightly higher f_T , as shown in Fig. 10. These results confirm that SiGe profiles optimized for high β and high

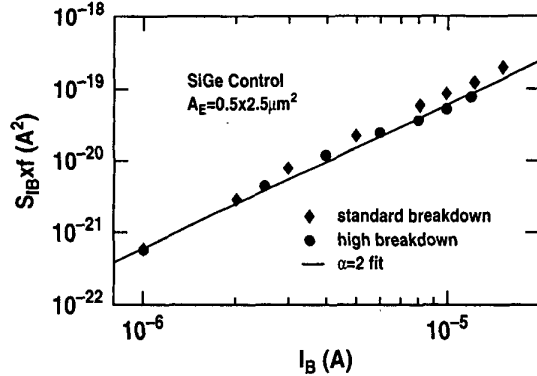


Fig. 5. Measured $S_{I_B} \times f$ product as a function of I_B for the standard and high breakdown voltage SiGe control HBTs. $A_E = 0.5 \times 2.5 \mu\text{m}^2$.

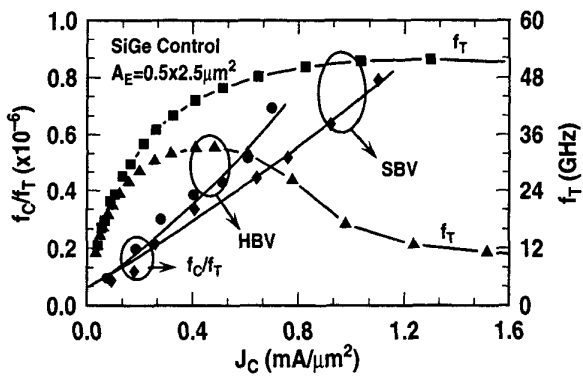


Fig. 7. Measured and modeled f_C/f_T ratio (left) and measured f_T (right) for the standard and high breakdown voltage SiGe control HBTs.

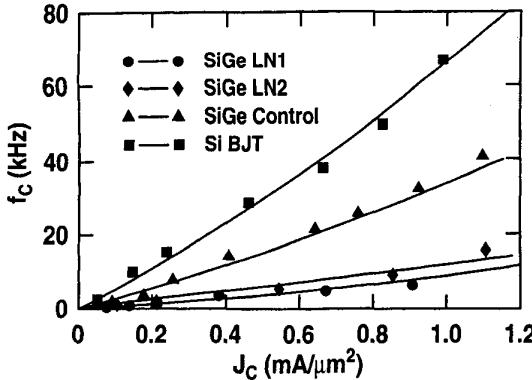


Fig. 8. Measured f_C as a function of J_C for the standard breakdown voltage Si BJT, SiGe control and two low-noise HBTs.

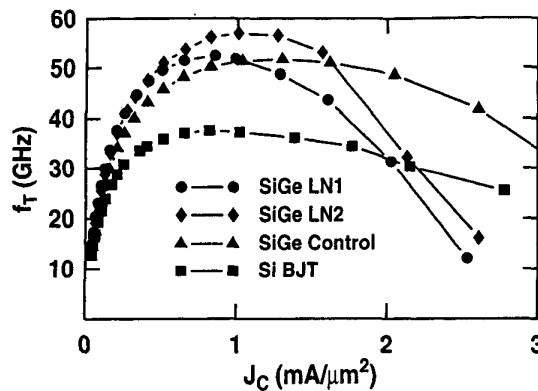


Fig. 9. Measured f_T as a function of J_C for the standard breakdown voltage Si BJT, SiGe control and two low-noise HBTs.

f_T have better phase noise performance for the same operating frequency. To achieve the same RF gain, a higher f_T transistor can operate at a lower J_C , thus reducing f_C/f_T , which further reduces f_C .

The above results suggest that the τ_f/β ratio can be used as a figure-of-merit for SiGe profile optimization, because f_C/f_T is proportional to $K\tau_f/\beta$ according to (4). The K factor is primarily determined by the emitter structure, and independent of the SiGe profile used in the base as well the collector doping profile, as evidenced by the experimental data. A SiGe profile producing the lowest τ_f/β ratio leads to the best f_C/f_T ratio, and has the best phase noise performance at higher frequencies.

The modeled f_C/f_T ratio for the Si comparision, SiGe control, and SiGe LN1 were calculated according to (4) which was derived using $\alpha = 2$. The α for SiGe LN2 (1.8), however, deviates from 2. The deviation is taken into account by using another f_C/f_T equation derived with α as a model parameter. This modified f_C/f_T equation was used to calculate the modeling curve for SiGe LN2. The modification is necessary to achieve good quantitative agreement with measurement for SiGe LN2. Eq. (4), however, provides better insight and intuitive understanding because of simple functional form.

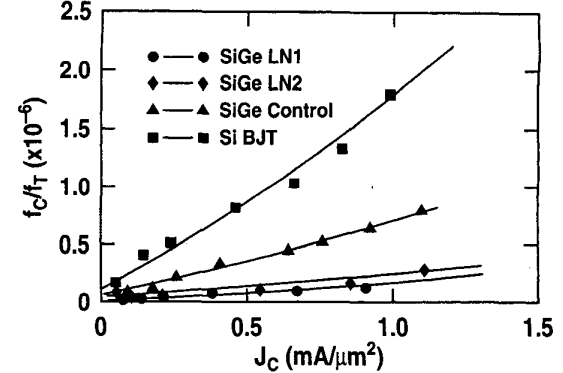


Fig. 10. Measured and modeled f_C/f_T ratio as a function of J_C for the standard breakdown voltage Si BJT, SiGe control and two low-noise HBTs.

V. CONCLUSIONS

We have presented modeling and experimental results of corner frequency (f_C) and corner frequency to cutoff frequency ratio (f_C/f_T) in a commercial SiGe HBT technology. The corner frequency f_C is proportional to the collector current density J_C and inversely proportional to β . The f_C/f_T ratio is proportional to the product of J_C , the forward transit time τ_f , the $1/f$ noise factor K , and inversely proportional to β . The high breakdown voltage devices designed for power amplifiers show nearly the same f_C and f_C/f_T ratio as the high f_T devices at lower J_C prior to the f_T rolloff. Measurements of devices featuring various SiGe profile designs show that both f_C and the f_C/f_T ratio can be significantly reduced by careful SiGe profile optimization without sacrificing SiGe film stability. The results also suggest that the τ_f/β ratio can be used as a $1/f$ noise figure-of-merit for SiGe profile and collector doping profile optimization in device design.

ACKNOWLEDGMENTS

This work was supported by the National Science Foundation under ECS-0119623 and ECS-0112923, the Semiconductor Research Corporation under SRC #2001-NJ-937 and # 2000-HJ-769, an IBM Faculty Partnership Research Award, and the Alabama Microelectronics Science and Technology Center. The wafers were fabricated at IBM Microelectronics, Essex Junction, VT. We would like to thank D. Ahlgren, S. Subbanna, D. Herman, B. Meyerson, and the IBM SiGe team for their contributions.

REFERENCES

- [1] D. Harame *et al.*, "Current status and future trends of SiGe BiCMOS Technology," *IEEE Trans. Electron Devices*, vol. 48, no. 11, pp. 2575-2594, 2001.
- [2] L. Vempati *et al.*, "Low-frequency noise in UHV/CVD epitaxial Si and SiGe bipolar transistors," *IEEE Journal of Solid-State Circuits*, vol. 31, no. 10, pp. 1458-1467, 1996.
- [3] B. Van Haaren *et al.*, "Low-frequency noise properties of SiGe HBT's and application to ultra-low phase-noise oscillators," *IEEE Transactions on Microwave Theory and Techniques*, vol. 46, no. 5, pp. 647-652, 1998.
- [4] L. K. J. Vandamme and G. Trefan, "Review of low-frequency noise in bipolar transistors over the last decade," *Proc. IEEE BCTM*, pp. 68-73, 2001.
- [5] D.C. Ahlgren *et al.*, *Tech. Dig. IEDM*, pp. 859-862, 1996.
- [6] G.F. Niu *et al.*, "SiGe profile design tradeoffs for RF circuit applications," *Tech. Dig. IEDM*, pp. 573-576, 1999.
- [7] G.F. Niu *et al.*, "Noise modeling and SiGe profile design tradeoffs for RF applications," *IEEE Trans. Electron Devices*, pp. 2037-2044, 2000.